

1 **Supercritical impregnation of polymer matrices spatially confined in**  
2 **microcontainers for oral drug delivery: effect of temperature, pressure**  
3 **and time**  
4

5 Marizza P.<sup>1</sup>, Pontoni L.<sup>2</sup>, Rindzevicius T.<sup>1</sup>, Alopaeus J. F.<sup>3</sup>, Su K.<sup>3</sup>, Zeitler A.<sup>3</sup>, Keller S. S.<sup>1</sup>, Kikic I.<sup>2</sup>,  
6 Moneghini M.<sup>4</sup>, De Zordi N.<sup>2</sup>, Solinas D.<sup>2</sup>, Cortesi A.<sup>2</sup>, Boisen A.<sup>1</sup>.

7 <sup>1</sup> Department of Micro- and Nanotechnology, Technical University of Denmark, Ørsteds Plads  
8 345E, 2800, Kongens Lyngby, Denmark.

9 <sup>2</sup> Department of Engineering and Architecture, University of Trieste, Piazzale Europa, I-34127,  
10 Trieste, Italy.

11 <sup>3</sup> Department of Chemical Engineering and Biotechnology, University of Cambridge, Pembroke  
12 Street, CB2 3RA, Cambridge, United Kingdom.

13 <sup>4</sup> Department of Chemical and Pharmaceutical Sciences, University of Trieste, Piazzale Europa, I-  
14 34127, Trieste, Italy.

15  
16 Keywords: supercritical fluids, impregnation, microcontainer, drug delivery, ketoprofen, PVP,  
17 poorly soluble drugs

18 **Abstract**

19 The present study is aimed to enhance the oral bioavailability of ketoprofen by inserting it into the  
20 matrix of poly(vinylpyrrolidone) (PVP) K10, a water soluble polymer, spatially confined into  
21 microcontainers, by means of supercritical CO<sub>2</sub>-aided impregnation. Microcontainers are  
22 cylindrical reservoirs, with typical sizes in the micrometer range, with a cavity open on one side,  
23 where the drug formulation is loaded. Differently to traditional tablets, microcontainers have a  
24 higher surface area per unit volume, and release the drug only in one direction. This design is  
25 meant to enhance the absorption of problematic drugs, like those with poor solubility in water. In  
26 a previous study we introduced a novel technique for drug loading of microcontainers, based on  
27 inkjet printing and supercritical impregnation (SCI). We showed that SCI produces accurate and  
28 reproducible drug loading for large arrays of microcontainers. In the attempt of enhancing the  
29 throughput of the loading methods, we propose the replacement of polymer inkjet printing with  
30 an easier manual compression of the PVP powder into the microcontainers. As the second step,  
31 the polymer powder filled-microcontainers were submitted to SCI. The separate role of different  
32 impregnation parameters (temperature, pressure, time, drug concentration in the supercritical  
33 phase) was elucidated with respect to the loading capacity. The microcontainer filling was  
34 observed by means of optical macroimaging, X-ray microtomography and scanning electron  
35 microscopy. The physical state of the drug was investigated by means of Raman spectroscopy and  
36 compared with selected representative PVP-ketoprofen physical mixtures. Finally, the drug loading  
37 was estimated by means of *in vitro* dissolution tests.

38 The characterization study shows that the present loading method is a valuable alternative to the  
39 one previously described. The drug loading can be controlled with high accuracy and  
40 reproducibility and the impregnated drug is in amorphous state. These results demonstrate that  
41 SCI can be used as a high throughput loading technique for microfabricated devices for oral drug  
42 delivery.

## 43 **1. Introduction**

44 Among the different drug delivery routes oral administration is still the most preferred one for its  
45 simplicity, minimal invasiveness, and high patient compliance. Nevertheless, the human digestive  
46 system presents a sequence of physiological barriers which drastically reduce the bioavailability of  
47 many active pharmaceutical ingredients (API): enzymatic degradation, hydrolysis in the gastric  
48 acidic environment, thick mucus layer covering the intestinal mucosa, selective transport action of  
49 peptide receptors in the epithelial cells [1]. Such unfavorable conditions are affecting APIs that  
50 exhibit low solubility in water. The solid state properties of drugs have a strong influence on their  
51 solubility. Whilst amorphous drug candidates exhibit an enhanced solubility and dissolution rate  
52 compared to their crystalline counterparts, amorphous forms often suffer from rather short  
53 thermodynamic stability and they spontaneously tend to crystallize [2]. As a result, stabilization of  
54 amorphous forms is necessary in order to preserve the abovementioned advantages [3]. Physical  
55 stabilization of the amorphous form can be achieved by the addition of a polymeric carrier  
56 wherein the drug is confined in supramolecular domains or even molecularly dispersed [4].  
57 Together with the solid state properties, the solubility and dissolution rate can be improved by  
58 reducing the particle size of the formulation [5]. Among the several formulation approaches [6]  
59 supercritical fluid based technology is a promising technique to produce micro- and  
60 nanoparticulated systems with high drug dispersion and enhanced stability and dissolution  
61 properties [7].

62 Beside the properties of the drug formulation, an important role in the therapeutic performance is  
63 often played by the design of the administration form. Conventional oral dosage forms like tablets  
64 provide a omni-directional drug release through their limited interfacial area when exposed to the  
65 physiological fluids. Furthermore, drug release from tablets is often slow compared to the  
66 peristaltic flow in the GI tract, which is the most permeable tissue for drug absorption. As a result,  
67 a large amount of API is not delivered, and patients need to ingest multiple drug doses to receive  
68 the desired therapeutic benefit. This increases the occurrence of potentially harmful side effects in  
69 patients [8].

70 In the last 10 years advances in field of micro- and nanofabrication have allowed the development  
71 of alternative drug delivery systems [9]. In particular there has been an increasing interest in  
72 microfabricated devices based on the concept of microcontainers [10]. A microcontainer is a  
73 reservoir with the typical dimensions falling in the micrometer range, composed by a non-  
74 permeable and inert shell and a cavity for the drug formulation open on one side from which the  
75 drug is released unidirectionally. Several groups developed microcontainers in different shapes,  
76 materials and designs, where fabrication is typically performed on flat silicon chips. By virtue of its  
77 asymmetric shape and by applying appropriate bioadhesive coatings on microcontainers Ainslie *et*  
78 *al.* [11] showed an increased intestinal retention time for these microdevices and an enhanced  
79 bioavailability for a model poorly water soluble drug. One of the big challenges in the fabrication  
80 of microcontainers concerns the drug loading step. In a previous work [12], we showed the  
81 fabrication of cylindrical microcontainers, fabricated with the epoxy resin SU-8. The microwells  
82 were filled with poly(vinylpyrrolidone) (PVP) by inkjet printing. This method showed high accuracy  
83 and a minimal waste of materials. In a more recent work [13] we proposed the combination of  
84 inkjet printing and supercritical technology to impregnate the polymer-filled microcontainers with  
85 ketoprofen, a poorly water soluble drug. We demonstrated that the supercritical impregnation  
86 technique allows a highly accurate and reproducible drug loading of large arrays of  
87 microcontainers. In an attempt to enhance the throughput of this loading method, we propose a  
88 simplified variant of our previous work. Here the polymer printing was replaced by an easier filling  
89 method, consisting of a manual compression of the polymer powder onto the microcontainer.  
90 Later, the powder filled-containers were submitted to supercritical impregnation (SCI) as  
91 previously described [13]. This process modification enabled a significant reduction in the sample

92 preparation time and made it possible to investigate the effect of temperature, pressure and  
93 impregnation times on different aspects concerning the drug loading in more detail.  
94 The loading procedure was characterized with different techniques. X-ray microtomography was  
95 used to measure the level of filling and the polymer morphology of the polymer powder in the  
96 microreservoir cavities before and after the SCI. In addition, microcontainers were visualized by  
97 scanning electron microscopy (SEM) to observe the effect of the impregnation parameters on the  
98 polymer morphology. Raman spectroscopy was used to investigate the drug solid state in the  
99 impregnated matrices and drug-polymer interactions. Finally, *in vitro* dissolution tests were  
100 carried out and the total drug loading was estimated. The results showed that the replacement of  
101 inkjet printing with the powder filling method enhances the throughput of the microcontainer  
102 loading technique without compromising the accuracy or the reproducibility of the whole loading  
103 process.

## 104 2. Materials and methods

### 105 2.1 Fabrication of SU-8 microcontainers

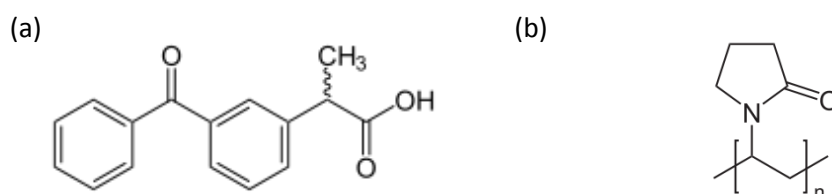
#### 106 2.1.1 Materials and fabrication of microcontainers

107 Silicon wafers (4-inch b100N n-type) were supplied by Okmetic (Vantaa, Finland). SU-8 2075 and  
108 SU-8 developer were purchased from Microresist Technology GmbH (Berlin, Germany).  
109 Cylindrical microcontainers were fabricated with a similar procedure as previously described [12].  
110 The microwells were fabricated with the epoxy-based photoresist SU-8 on silicon wafers arranged  
111 in a squared chip containing an array of 25x25 microcontainers. A microcontainer has a cavity of  
112 approximately 300  $\mu\text{m}$  in diameter and 270  $\mu\text{m}$  in depth and an approximated volume of 18 nL.  
113 After the fabrication the wafer was cut into square chips containing 625 microcontainers (DISCO  
114 DAD 321, Automatic Dicing Saw).

### 115 2.2 Drug loading of microcontainers

#### 116 2.2.1 Materials

117 Ketoprofen (98%, racemate) and polyvinylpyrrolidone (PVP K10, Mw 10,000) were supplied by  
118 Sigma Aldrich. Carbon dioxide was supplied by SIAD (99% purity). Ketoprofen is a nonsteroidal  
119 anti-inflammatory drug (NSAID) with analgesic and antipyretic properties. In several  
120 pharmacopoeias ketoprofen is considered as practically insoluble in water [14]. Its solubility in  
121 pure water at room temperature (22-24°C) was reported to be 0.010 mg/mL [15]. Thus,  
122 ketoprofen is classified as a class II active principle in the biopharmaceutical classification system  
123 (BCS): It exhibits low aqueous solubility and a high intestinal permeability.



129 Figure 1: Chemical structure of (a) ketoprofen, (b) monomer of poly (vinyl  
130 pyrrolidone) (PVP).

131 2.2.2 Filling with poly(vinylpyrrolidone) PVP powder

132 Microcontainers were filled with PVP powder with the following procedure: the powder was  
133 deposited and compacted with a spatula onto the microwells and the residual amount, placed in  
134 between containers, was blown away by means of a pressurized air. The chip was weighed before  
135 and after filling and the average PVP weight per chip was estimated. The level of microcontainer  
136 filling was measured by X-ray microtomography in different positions of the chip.

137 2.2.3 Supercritical impregnation of polymer filled-microcontainers

138 After the powder deposition the drug was loaded into the polymer-filled microdevices by means  
139 of supercritical carbon dioxide impregnation. Figure 1.2 depicts a schematic of the high pressure  
140 setup used in the impregnation experiments. The operation was performed in a 100 mL reactor  
141 (KM 20-05 autoclave NWA, Germany) equipped with a magnetic stirrer drive (Mrk MINI 100)  
142 assembled in a sealed housing directly threading into the reactor head. During the impregnation  
143 experiments the reactor was fed with liquid CO<sub>2</sub> through an on/off valve (V1) by a high pressure  
144 pump (PM-101NWA, NWA, Germany). At the end of the experiments the reactor was slowly  
145 emptied through an on/off purge valve followed by a lamination valve (V2) and the outlet stream  
146 was connected to a deflux flask where the gaseous CO<sub>2</sub> was bubbled through an ethanol solution  
147 (95%) and the ketoprofen concentration was measured. The resulting drug solution was made up  
148 to defined volumes and the drug content was estimated by UV spectroscopy measurements  
149 (Thermo Scientific Evolution 60 - Thermo Fisher Scientific Inc.). Finally, the drug free-CO<sub>2</sub> stream  
150 was connected to a flowmeter (SIM Brunt, Italy).

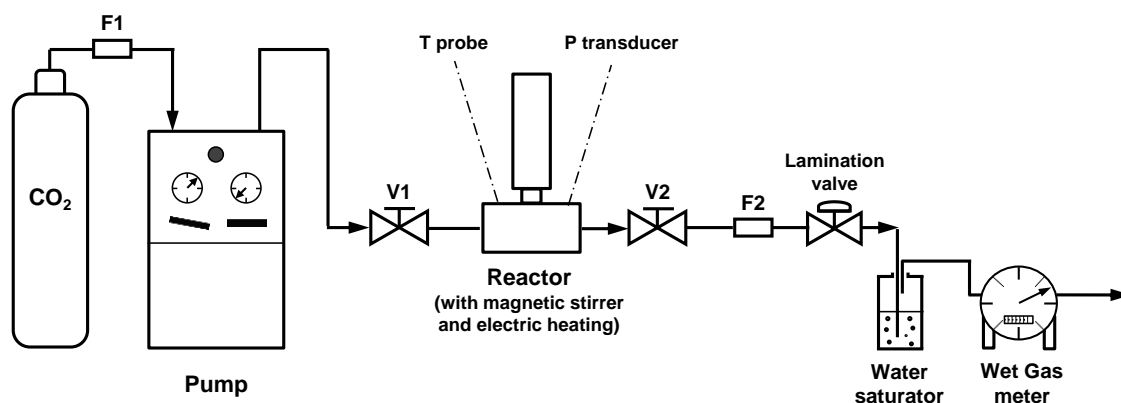


Figure 2: Schematic of the high pressure plant. F<sub>i</sub> and V<sub>i</sub> indicate 0.5 µm filters and on/off valves.

151  
152 The impregnation experiments were carried out in batch conditions with defined steady-state  
153 values of CO<sub>2</sub> pressure, temperature and stirring velocity. In each batch, weighted amounts of  
154 crystalline ketoprofen powder and one chip were placed in separate compartments of a sample  
155 carrier placed at the bottom of the reactor. In order to avoid damage to the microcontainers  
156 during the chamber filling with the supercritical fluid, the back of the chips were glued onto the  
157 sample carrier with a carbon pad tape. The reactor was then sealed and heated to the defined  
158 temperature. When the set point temperature was achieved, the inlet valve was gradually opened  
159 and the chamber was slowly filled with CO<sub>2</sub>, in order to maintain isothermal conditions and avoid  
160 turbulence within the reactor, which could result in detachment of the chip and damaging of the  
161 microcontainers. When the desired pressure was achieved, the inlet valve was closed and the  
162 stirrer was switched on. During the experiment the supercritical CO<sub>2</sub> phase dissolved the solid drug  
163 powder and swelled the polymer within the microcontainers. The drug was therefore physically

164 conveyed and loaded in the polymer matrices. The impregnations were carried out at a fluid  
165 pressure of 100 and 200 bar, temperatures of 40, 50 and 60°C and durations of 1 and 4 hours with  
166 a stirring velocity of 20 rpm, respectively.

167 In the experiments run at 100 bar the drug was dissolved under saturation conditions according to  
168 the solubility values of ketoprofen in supercritical CO<sub>2</sub> reported by Macnaughton et al. [16] at the  
169 chosen conditions of temperature. In this group of experiments the temperature and time were  
170 modified from batch to batch. Because of the batch conditions, the drug concentration could not  
171 be kept at solubility value over time. In contrast, in the tests performed at 200 bar a fixed amount  
172 of ketoprofen was dissolved, corresponding to the saturation concentration of the compound at  
173 200 bar and 40°C. At 200 bar and 50°C and 60°C the amount of drug was dissolved under  
174 saturation conditions, as the solubility values are higher at these temperatures. In the experiment  
175 performed at 200 bar, the exclusive effect of temperature and time on the microcontainer  
176 impregnation was studied. At the end of the experiment the reactor was depressurized at a  
177 controlled rate for approximately 2 and 3 hours when the operating pressures were 100 and 200  
178 bar respectively. After the experiments the chips were stored in a desiccator until further analysis  
179 were performed. In Table 1 the operating conditions of the experiments are shown.

180

181 Table 1: Mass of ketoprofen [mg] dissolved in the different experimental conditions

Pressure [bar]	Temperature [°C]		
	40	50	60
100	4.83	2.15	1.31
200	14.1	14.1	14.1

182

## 183 2.3 Characterization methods

### 184 2.3.1 X-ray microtomography (X $\mu$ CT)

185 For the X $\mu$ CT measurements a Skyscan 1172/F instrument (Skyscan, Kontich, Belgium, control  
186 software v1.5.13) was used. A source voltage of 60 kV and current of 165  $\mu$ A were used together  
187 with a 0.5 mm thick Al filter to attenuate the high energy X-rays. For each sample 780 shadow  
188 images were acquired over 180° of rotation. The resulting data acquisition time was 4 h for each  
189 sample. Reconstruction of the cross-section images was performed using the program  
190 NRecon+GPUReconServer (Skyscan, beta v1.6.5) on a single PC using GPU accelerated  
191 reconstruction (Windows 7 64-bit workstation, 2 Intel Xeon X5647 with 4 cores each, 48 GB RAM,  
192 NVIDIA quadro 4000 with 256 cores). Image reconstruction using the Feldkamp algorithm [17] for  
193 cone beam geometry took about 30 min per sample and resulted in, depending on sample size,  
194 about 1450 slices of 2864 x 2876 pixels each (5.2  $\mu$ m isotropic voxel size). Using the DataViewer  
195 (Skyscan, v1.4.4) the tablet was rotated to align the microwells parallel to the x-axis.

196

### 197 2.3.2 Scanning electron microscopy (SEM)

198 The morphology of the impregnated microcontainers was examined using SEM. The investigations  
199 were carried out using a Nova600 NanoSEM from FEI (Eindhoven, the Netherlands). Imaging was  
200 performed in low-vacuum-mode at a pressure of 0.6 mbar and an operation voltage of 5 kV. Prior  
201 to examination, the samples were mounted onto metal stubs and were tilted by approx. 30  
202 degrees.

203

### 204 2.3.3 Raman spectroscopy

205 As described in a previous study [13], Raman spectroscopy can be used to elucidate the presence  
206 of chemical interactions amongst drug molecules and between drug and polymer. The spectra  
207 from the impregnated microcontainers were collected using a Thermo Scientific Raman DXR  
208 microscope equipped with a frequency-stabilized single mode diode laser. The Raman signal  
209 collection time was 5 sec and the signal was averaged three times, using a 25  $\mu\text{m}$  slit and a 1.0  $\mu\text{m}$   
210 diameter laser post. The Raman DXR microscope was coupled to a single grating spectrometer  
211 with a 5  $\text{cm}^{-1}$  FWHM spectral resolution and a  $\pm 2 \text{ cm}^{-1}$  wavenumber accuracy. All Raman spectra  
212 were recorded at a laser power of 10 mW, using a 10X objective lens and a laser excitation  
213 wavelength of 780 nm. In each sample 5 containers, located at different positions on the chip,  
214 were selected and analyzed. The intrinsic fluorescence background was fitted to a polynomial  
215 function and subtracted from the collected signal.

### 216 2.3.4 In vitro drug dissolution studies

217 Dissolution of PVP and ketoprofen from loaded microcontainers was determined in 10 ml DI water  
218 at 37° C using a UV spectrophotometer  $\mu\text{DISS}$  profiler (Pion, USA). Individual chips were glued with  
219 carbon pads on teflon-coated magnets which stirred at 100 rpm. For the detection of ketoprofen,  
220 the wavelength was set to 259 nm. After dissolution, the microcontainers were observed with an  
221 optical microscope (Zeiss, Germany, 10x magnitude) to confirm complete emptying. The amount  
222 of drug loaded per chip was estimated by the final concentration measured in the dissolution test  
223 at 16 hours. Solubility of ketoprofen at 37 °C in aqueous solutions changes significantly with pH  
224 between 1 and 7 [14]. Nevertheless, even in the test with the highest drug loading, the pH of the  
225 dissolution medium drop below 6.5 as ketoprofen is a weak acid ( $\text{pK}_a$  4.5). Therefore, according to  
226 solubility data reported in the literature [14], the dissolution tests were performed in conditions  
227 below saturation that is without drug precipitation, which was also confirmed by the non-  
228 decreasing monotonic trend of the drug dissolution profiles (data not shown).

## 229 3. Results and discussion

### 230 3.1 Polymer filling of microcontainers and X-ray microtomography

231 A picture of arrays of microcontainers filled with PVP powder is shown in Figure 3. The powder  
232 filling required few seconds to be performed and resulted in an accurate deposition inside the  
233 cylindrical cavities of the microwells, with minimal residues in between, as representatively  
234 illustrated by the high color contrast between the dark silicon surface and the brilliant white of  
235 PVP powder. In Figure 4 a scanning electron microscopy image of microcontainers filled with PVP  
236 powder is reported. The polymer granules are compacted inside the microwells and this  
237 confinement prevents them from being removed by the air flow which is used to remove the loose  
238 powder after the filling step.. Figure 5 shows the cross-sections that were reconstructed from the  
239 microtomography data of the  $\text{X}\mu\text{CT}$  measurements. Using this technique it is possible to measure  
240 the internal microstructure of the PVP powder within the containers and to visualise the effect of  
241 the impregnation on the particle morphology. The images clearly show that the microcontainers  
242 are filled with discrete PVP particles before impregnation and subsequently coalesce following  
243 treatment with supercritical  $\text{CO}_2$ .

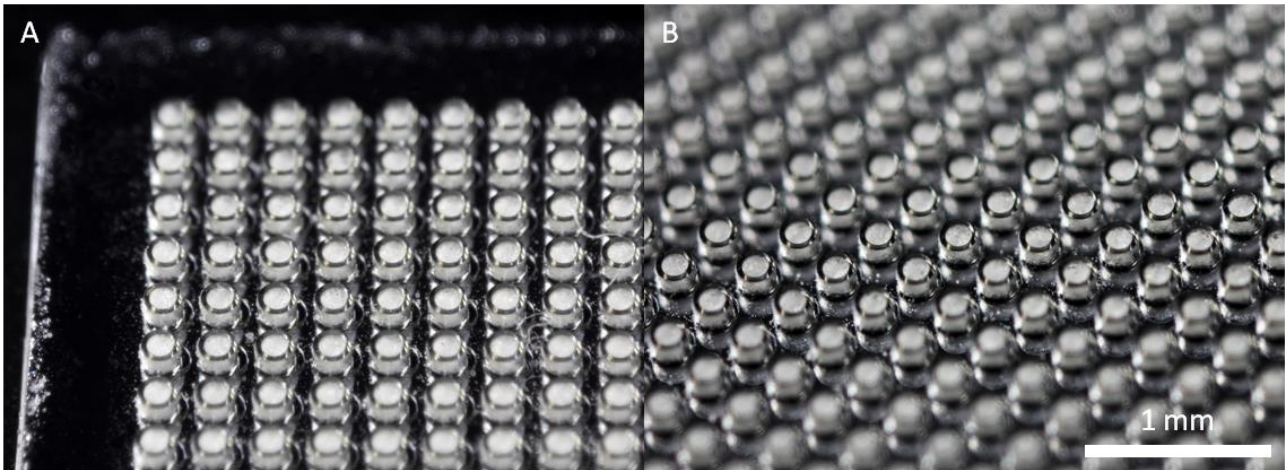


Figure 3: Optical macro images of microcontainers filled with PVP powder by manual compaction: (a) detail of the chip corner, (b) arrays in the middle of the chip.

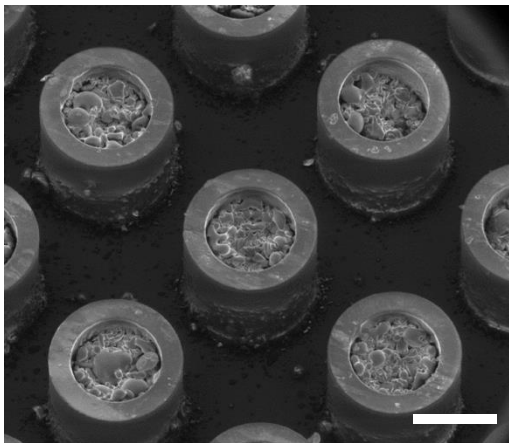


Figure 4: SEM images of microcontainers filled with polyvinylpyrrolidone before treatment with supercritical CO<sub>2</sub>. The scalebar indicates 300 μm.

244

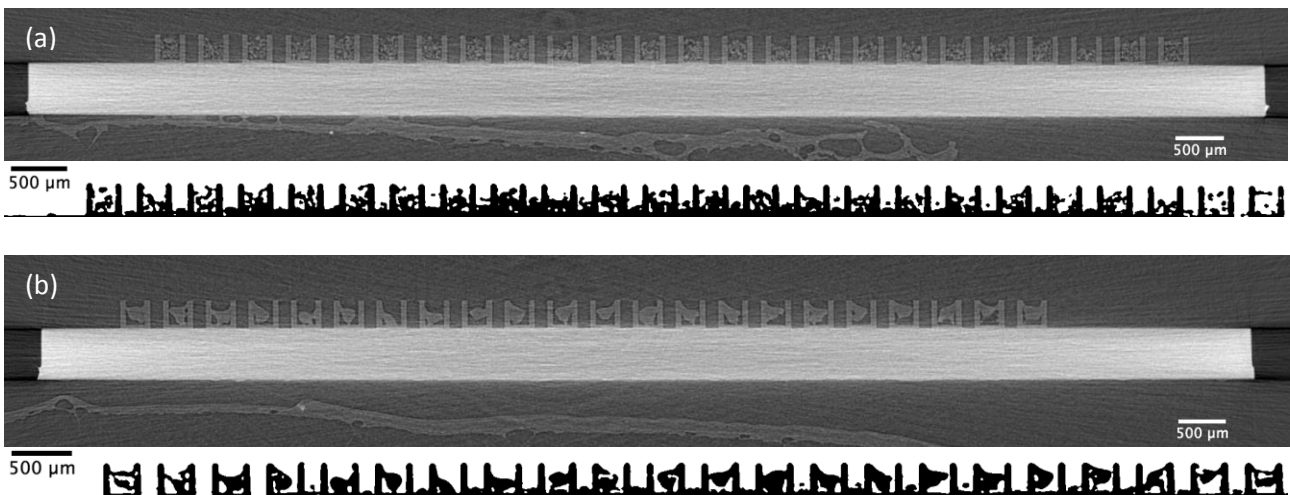


Figure 5: Non-destructive cross-sections acquired by XμCT through the microcontainers filled with polyvinylpyrrolidone before treatment with supercritical CO<sub>2</sub> (a) and after impregnation (b). The original grey scale images are shown together with a binary threshold image to highlight the change in polymer morphology.

245

### 246 3.2 Scanning Electron Microscopy of impregnated microcontainers

247 After the supercritical treatment, the microcontainers were analyzed by scanning electron  
248 microscopy to observe the effects of the impregnation on the polymer morphology. As shown in a  
249 previously [13], the SEM micrographs (see Figure 6) confirm that scCO<sub>2</sub> does not visible effects on  
250 the epoxy resin used to fabricate the microcontainers (SU-8) which maintain their size, the  
251 cylindrical shape and the adhesion to the silicon substrate. The supercritical fluid has instead a  
252 much more pronounced effect on PVP. At all the tested conditions, the morphology of PVP  
253 radically changes as the polymer particles undergo swelling and subsequent coalescence as  
254 confirmed by the X $\mu$ CT images (Figure 5b). By comparing the SEM micrographs of microcontainers  
255 treated at different pressures it is clear that the volume of the polymer visibly increases with  
256 increasing CO<sub>2</sub> pressure. This can be explained by an increase of CO<sub>2</sub> uptake in PVP with pressure,  
257 in accordance with what was previously reported by Kikic and co-workers [18]. At high pressures,  
258 CO<sub>2</sub> has a well-known plasticizing effect on certain polymers [19,20]. The plasticization leads to a  
259 drop in the T<sub>g</sub>, which for PVP K10 is around 87 °C, a temperature close to the operating  
260 temperature during impregnation. As a result, the polymer gets close to the glass-rubber  
261 transition. The increase of impregnation time in general leads to a higher extent of swelling of the  
262 matrix and to the appearance of holes. At 40 °C and 50 °C these holes got larger when the pressure  
263 was set at 200 bar, and this fact can be attributed to the release of CO<sub>2</sub> from the highly swollen  
264 matrices. At 200 bar and 50 °C small spots appear on the polymer surface. At 200 bar and 60 °C  
265 these particles clustered in bigger aggregates (see Figures 6(k) and 6(l)) on small number of  
266 containers in the chip. As scCO<sub>2</sub> acts as a plasticizer for polymers the viscosity of the CO<sub>2</sub> saturated  
267 matrix decreases during impregnation [34] causing spillages, in some cases, from the containers.  
268 This aspect is more pronounced during longer experiments.  
269

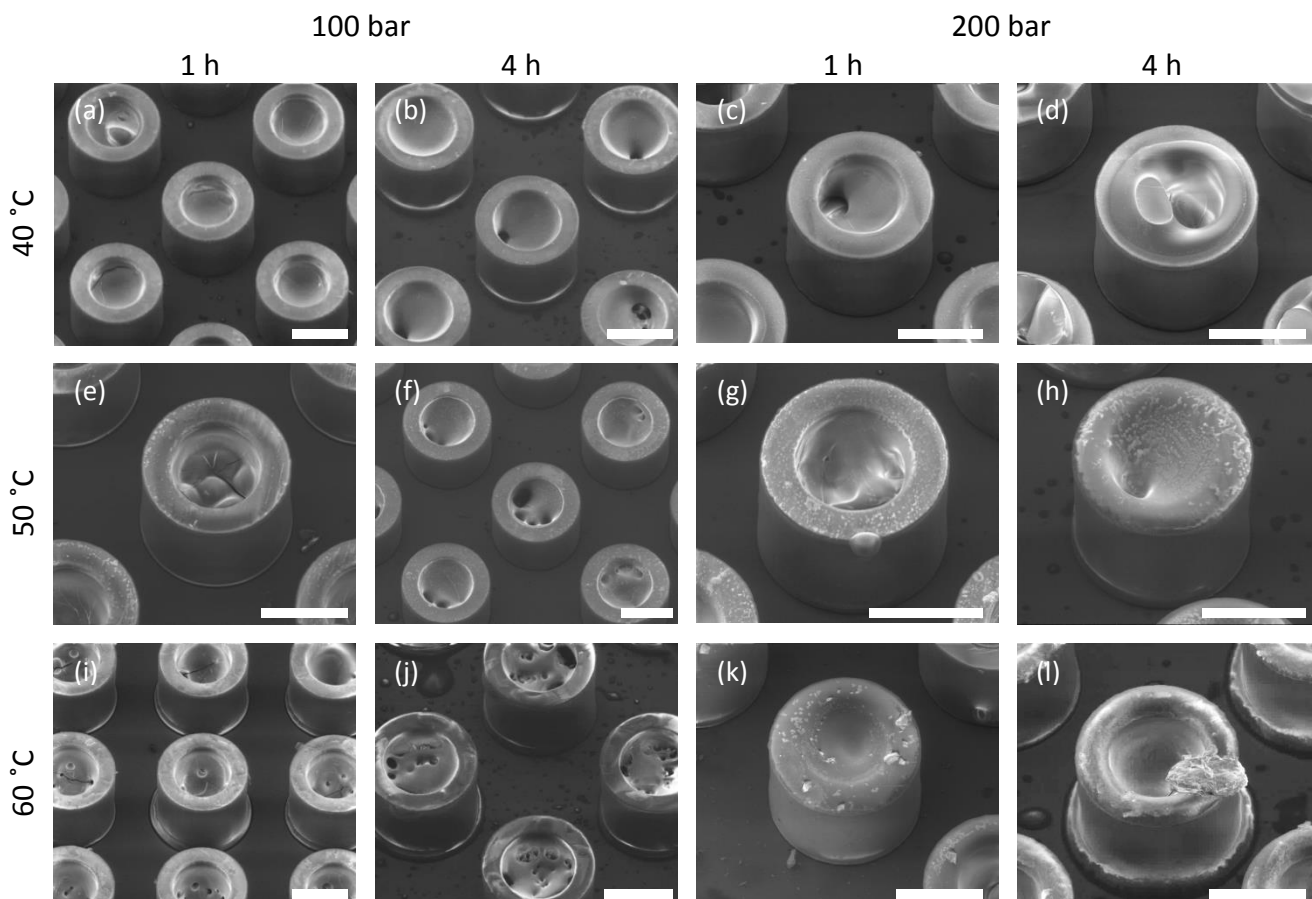


Figure 6: Scanning electron microscopy images of polymer filled microcontainers impregnated with ketoprofen by supercritical CO<sub>2</sub> at different pressure, temperature and time. The scalebar indicates 300 μm.

270

### 271 3.3 Loading of ketoprofen into polymer filled-microcontainers

272 The solubility of ketoprofen in scCO<sub>2</sub> monotonically increases with the fluid density, and therefore  
273 with the fluid pressure at isothermal conditions [16]. Furthermore, for many active compounds  
274 under isobaric conditions the temperature influences the solubility according to the operating  
275 pressure and with respect to the crossover pressures. At the crossover points solubility isotherms  
276 overturn their trend [16]. The upper crossover pressure of ketoprofen in carbon dioxide was  
277 measured between 160 and 180 bar [18,21]. Below this pressure, such as at 100 bar, the drug  
278 solubility decreases with temperature. At higher pressures, such as at 200 bar, the effect of  
279 temperature is the opposite. The impregnation pressures were chosen on different positions  
280 towards the upper crossover point in order to explore the behavior of the supercritical phase on  
281 the drug loading. In figure 7 the resulting weight fraction of ketoprofen ( $\omega_{\text{ketoprofen}}$ ) loaded in a chip  
282 containing 625 PVP filled-microcontainers is compared for the different impregnation conditions.  
283 Despite the simplicity of the method the overall accuracy of the loading is similar to the one  
284 previously reported where the polymer was deposited by inkjet printing [12].

285 In the tests carried out at 100 bar (Figure 7a) the drug was dissolved in saturation conditions. Here  
286 the loading is strongly dependent on the drug concentration in the supercritical phase, which was  
287 higher at 40°C and lower at 60°C. There is an increase in drug loading over time for any tested  
288 temperature meaning that after 1 hour the equilibrium is not yet attained. After 4 hours the drug  
289 weight fraction is approximately doubled at all temperatures. To investigate the partition  
290 equilibrium of the drug between the CO<sub>2</sub> and the polymer phases an impregnation experiment  
291 was carried out at 40°C for 24 hours. The attained drug fraction was 0.27, which is very close to  
292 the loading achieved after 4 hours. In the experiments at 200 bar, the impregnation is enhanced  
293 compared to experiments at 100 bar as a result of the combined effect of the higher amount of  
294 drug dissolved (see table 1) and the density of the fluid at this pressure. However, at 200 bar the  
295 loading increased with the temperature which was unexpected, since at this pressure a rise of  
296 temperature leads to an increase of drug solubility and therefore a less favorable drug partition in  
297 the polymer matrix. Moreover, from 40 °C to 60 °C the fluid density decreases as shown in the  
298 profiles in Figure 8, where the loaded API weights are plotted as a function of the CO<sub>2</sub> density.  
299 These latter results can be explained by considering that the effect of temperature on drug-scCO<sub>2</sub>  
300 diffusivity prevails over the reduced fluid density. A temperature increase also results in enhanced  
301 mobility of the polymer chains, which is suggested by the visible swelling observed in Figures 6(d),  
302 6(h) and 6(l). In contrast to the results at 100 bar, at 200 bar more limited loading gains for  
303 impregnation time were achieved. This might be due to the proximity of the drug concentration in  
304 the polymer to the saturation, which can slow down the impregnation process.

305

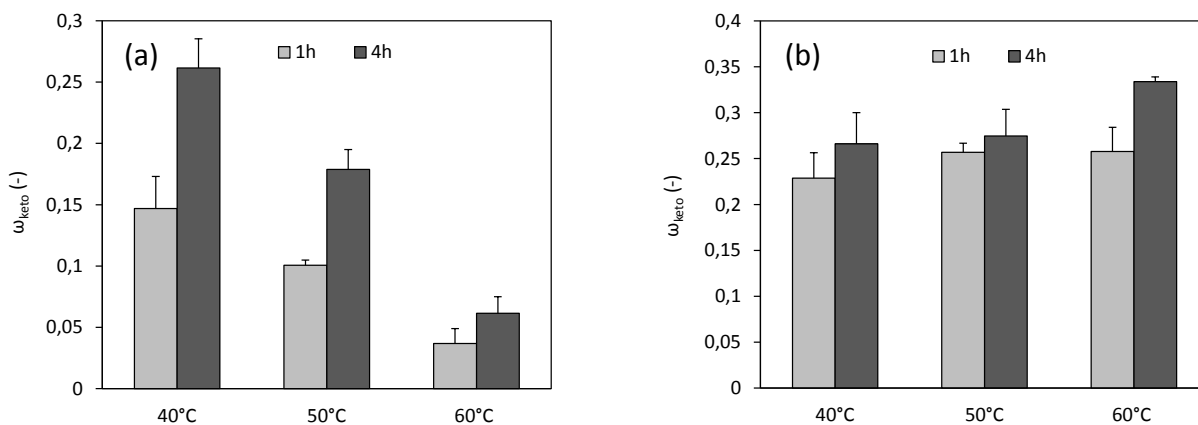


Figure 7: Mass fraction of ketoprofen ( $\omega_{keto}$ ) impregnated in polymer filled 625 microcontainers at different temperatures and times: (a) at 100 bar in saturation conditions (b) at 200 bar with a fixed amount of drug dissolved in  $scCO_2$  (N=3).

306

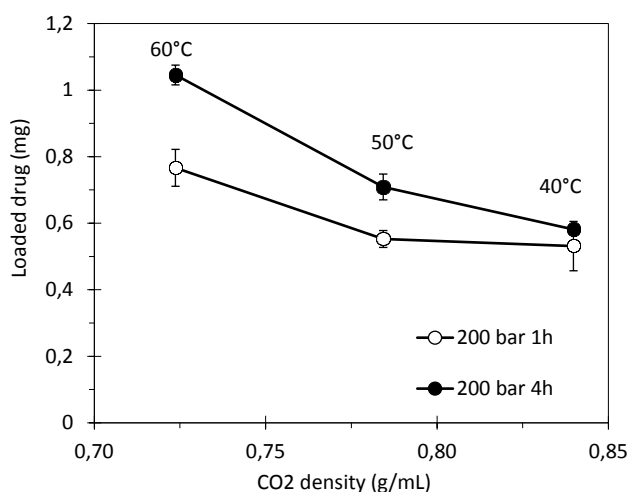


Figure 8: Mass of ketoprofen impregnated at 200 bar in 625 microcontainers at different temperatures and times (N=3) as function of the  $CO_2$  density.

307

308

309

310

Table 2: Drug loading of impregnated microcontainers. The drug weight refers to total loaded mass on individual chips (625 microcontainers) and is normalized with respect to the polymer mass in the microwells (N = 3).

T (C)	P(bar)	Time (h)	Loaded drug per chip (mg)	Drug weight fraction (keto/(PVP+keto))
40	100	1	0.33 ± 0.09	0.15 ± 0.03
		4	0.58 ± 0.02	0.26 ± 0.02
	200	1	0.53 ± 0.07	0.23 ± 0.03
		4	0.58 ± 0.01	0.27 ± 0.03
50	100	1	0.19 ± 0.02	0.10 ± 0.01
		4	0.40 ± 0.04	0.18 ± 0.02
	200	1	0.55 ± 0.03	0.26 ± 0.01
		4	0.71 ± 0.04	0.27 ± 0.03
60	100	1	0.08 ± 0.03	0.04 ± 0.01
		4	0.16 ± 0.04	0.06 ± 0.01
	200	1	0.77 ± 0.06	0.26 ± 0.03
		4	1.05 ± 0.03	0.33 ± 0.01

311

### 312 3.4 Raman spectroscopy

313 Another important aspect for a drug delivery device is the API solid state properties and the  
314 stabilization of the amorphous phase in a polymer matrix. For this purpose, Raman scattering  
315 spectroscopy was utilized to detect the presence of amorphous ketoprofen and the molecular  
316 interactions with the polymer. In order to elucidate the presence of drug-polymer interactions,  
317 additional Raman spectra were collected from microcontainers filled with physical mixtures (PMs)  
318 of the polymer and drug. Raman scattering spectra of both fresh ketoprofen:PVP PMs and  
319 mixtures prepared by supercritical CO<sub>2</sub> are shown in Figure 9. In the ketoprofen:PVP PM case, the  
320 Raman scattering spectra from both compounds are added together and retain all characteristics  
321 of isolated ketoprofen and PVP, see Figure 9(a). To illustrate this, the inter-ring ketoprofen  
322 carbonyl [C=O] stretching mode [22] found at 1657 cm<sup>-1</sup> is examined for different drug/PVP ratios.  
323 In all cases the Raman intensity of the ketoprofen C=O stretching mode compared to the 1602 cm<sup>-1</sup>  
324 C-C stretching mode is  $I_{1657}/I_{1602} > 1$ . The Raman vibration can be fitted to two Lorentzian  
325 functions outlining modes that belong to both ketoprofen and PVP. The FWHM of the C=O  
326 stretching mode is similar to the one recorded for pure ketoprofen shown in the bottom part of  
327 Figure 9(a). The PM result indicates no observable intermolecular interaction between the two  
328 compounds [13]. The 1657 cm<sup>-1</sup> Raman mode for supercritical CO<sub>2</sub> impregnated ketoprofen:PVP  
329 mixtures behaves differently, i.e. the vibrational mode intensity is reduced and the FWHM is  
330 significantly increased, see Figure 9(b). In this case, the two Lorentzian fits yield essentially a single  
331 Raman peak without a clear contribution from PVP and  $I_{1657}/I_{1602} < 1$  almost for all drug/PVP  
332 ratios. Since there is no observable frequency shift, the result suggests that this carbonyl group is  
333 not involved in the formation of hydrogen bonds with PVP molecules. The recorded change rather  
334 indicates rearrangement of ketoprofen molecules into a less organized solid state, and a similar  
335 effect was previously observed for aged ketoprofen:PVP PM mixtures [13]. The presence of  
336 amorphous ketoprofen was previously confirmed by X-ray diffraction [13]. It is also expected that  
337 the CO<sub>2</sub> assisted impregnation of PVP with ketoprofen breaks or reduces the interaction between  
338 adjacent ketoprofen molecules and induces the formation of the hydrogen bonds between oxydryl  
339 groups of ketoprofen molecules and carbonyl groups of PVP [23].

340

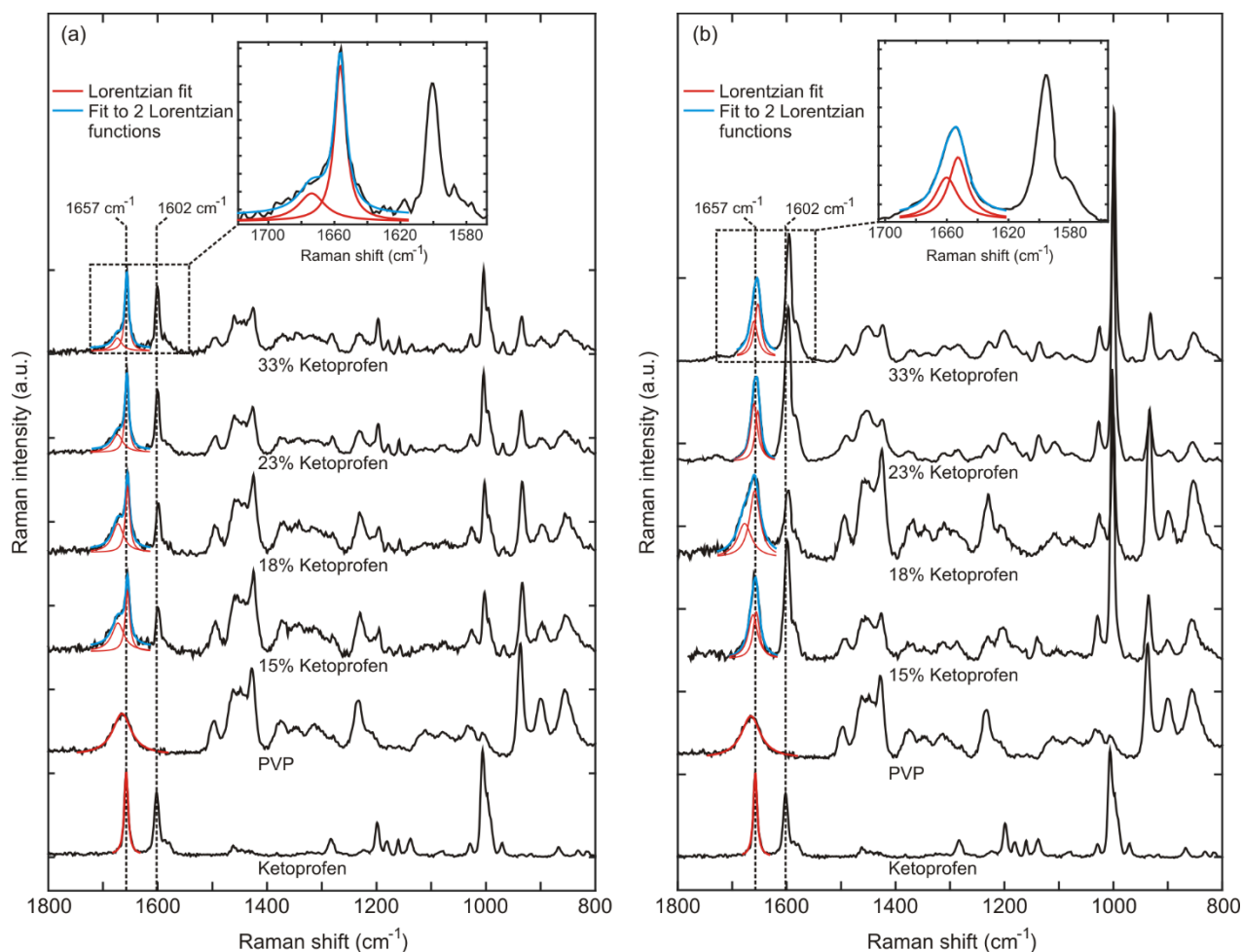


Figure 9: Raman spectra of (a) physical mixtures of PVP and crystalline ketoprofen in different representative weight percentages and (b) spectra of PVP impregnated with the same ketoprofen weight percentages at different experimental conditions (see table 2).

341

342

#### 4. Conclusions

343

344

345

346

347

348

349

350

351

352

353

354

355

356

357

358

359

360

361

The present study investigates the use of CO<sub>2</sub>-aided impregnation to load ketoprofen into microcontainers filled with PVP by tuning temperature, pressure, time, and drug concentration in the fluid phase. The characterization study shows that drug loading can be controlled with high accuracy and reproducibility and the impregnated drug is in the amorphous state. At any tested pressure there is an increase of drug loading over time for any tested temperature meaning that after 1 hour the equilibrium between the polymer and the CO<sub>2</sub> phases is not yet attained. From the tests at 100 bar it was observed that the loading is strongly dependent on the drug concentration in the impregnating medium. Unexpectedly, in the tests at 200 bar the loading increased with the temperature despite the increasing drug solubility in the scCO<sub>2</sub>. This was attributed to the predominance of drug diffusivity in the polymer matrix. In contrast, at 200 bar more limited loading gains for increasing impregnation time were obtained probably due to the proximity of drug saturation in the polymer. The Raman scattering spectra of the impregnated matrices indicate a rearrangement of ketoprofen molecules into a less organized state. However, no observable frequency shift in was noticed for the spectral modes typically ascribed to drug-polymer interactions, which suggests that the drug molecule is unlikely to be involved in the formation of hydrogen bonds with PVP molecules.

Our results demonstrate that the combination of powder loading and SCI can be used as a high throughput loading technique for microfabricated devices for oral drug delivery.

362 **5. Acknowledgements**

363 This project was developed within the Center for Intelligent Drug Delivery and Sensing Using  
364 Microcontainers and Nanomechanics (IDUN) Danmarks Grundforskningsfonds og Villum Fondens  
365 (Denmark). The authors would like to acknowledge support by the K. K. Engineering and Physical  
366 Science Research Council (EP/K503721/1). The authors also thank Prof. Mario Grassi (University of  
367 Trieste) for the fruitful discussions and the valuable inputs given to the research work.

368  
369 **5. Bibliography**

- 370 [1] B. Steffansen, C.U. Nielsen, B. Brodin, A.H. Eriksson, R. Andersen, S. Frokjaer, Intestinal  
371 solute carriers: an overview of trends and strategies for improving oral drug absorption, *Eur.*  
372 *J. Pharm. Sci.* 21 (2004) 3–16. doi:10.1016/j.ejps.2003.10.010.
- 373 [2] M. Yoshioka, B.C. Hancock, G. Zografi, Crystallization of indomethacin from the amorphous  
374 state below and above its glass transition temperature, *J. Pharm. Sci.* 83 (1994) 1700–1705.  
375 doi:10.1002/jps.2600831211.
- 376 [3] R. Laitinen, K. Löbmann, C.J. Strachan, H. Grohganz, T. Rades, Emerging trends in the  
377 stabilization of amorphous drugs., *Int. J. Pharm.* 453 (2013) 65–79.  
378 doi:10.1016/j.ijpharm.2012.04.066.
- 379 [4] E.B. Basalious, W. El-Sebaie, O. El-Gazayerly, Rapidly absorbed orodispersible tablet  
380 containing molecularly dispersed felodipine for management of hypertensive crisis:  
381 development, optimization and in vitro/in vivo studies., *Pharm. Dev. Technol.* 18 (2013)  
382 407–16. doi:10.3109/10837450.2012.659258.
- 383 [5] N. Rasenack, H. Hartenhauer, B.W. Müller, Microcrystals for dissolution rate enhancement  
384 of poorly water-soluble drugs, *Int. J. Pharm.* 254 (2003) 137–145. doi:10.1016/S0378-  
385 5173(03)00005-X.
- 386 [6] D.Z. Nicola, C. Angelo, K. Ireneo, M. Mariarosa, D. Solinas, Pharmaceutical and Nutraceutical  
387 Applications of Supercritical Carbon Dioxide, in: J. Osborne (Ed.), *Handb. Supercrit. Fluids*  
388 *Fundam. Prop. Appl.*, NOVA Science, New York, 2014: pp. 79–103.
- 389 [7] A. Martín, M.J. Cocero, Micronization processes with supercritical fluids: fundamentals and  
390 mechanisms., *Adv. Drug Deliv. Rev.* 60 (2008) 339–50. doi:10.1016/j.addr.2007.06.019.
- 391 [8] K.M. Woessner, M. Castells, NSAID single-drug-induced reactions., *Immunol. Allergy Clin.*  
392 *North Am.* 33 (2013) 237–49. doi:10.1016/j.iac.2012.12.002.
- 393 [9] F.J. Martin, C. Grove, Microfabricated Drug Delivery Systems: Concepts to Improve Clinical  
394 Benefit, *Biomed. Microdevices.* 3 (n.d.) 97–108. doi:10.1023/A:1011442024658.
- 395 [10] C.B. Fox, H.D. Chirra, T.A. Desai, Planar bioadhesive microdevices: a new technology for oral  
396 drug delivery., *Curr. Pharm. Biotechnol.* 15 (2014) 673–83.  
397 doi:10.2174/1389201015666140915152706.
- 398 [11] K.M. Ainslie, R.D. Lowe, T.T. Beaudette, L. Petty, E.M. Bachelder, T.A. Desai, Microfabricated  
399 devices for enhanced bioadhesive drug delivery: attachment to and small-molecule release

- 400 through a cell monolayer under flow., *Small*. 5 (2009) 2857–63.  
401 doi:10.1002/sml.200901254.
- 402 [12] P. Marizza, S.S. Keller, A. Boisen, Inkjet printing as a technique for filling of micro-wells with  
403 biocompatible polymers, *Microelectron. Eng.* 111 (2013) 391–395.
- 404 [13] P. Marizza, S.S. Keller, A. Müllertz, A. Boisen, Polymer-filled microcontainers for oral  
405 delivery loaded using supercritical impregnation, *J. Control. Release*. 173 (2014) 1–9.
- 406 [14] I.E. Shohin, J.I. Kulinich, G. V Ramenskaya, B. Abrahamsson, S. Kopp, P. Langguth, et al.,  
407 Biowaiver monographs for immediate-release solid oral dosage forms: ketoprofen., *J.*  
408 *Pharm. Sci.* 101 (2012) 3593–603. doi:10.1002/jps.23233.
- 409 [15] T. Loftsson, D. Hreinsdóttir, Determination of aqueous solubility by heating and  
410 equilibration: a technical note., *AAPS PharmSciTech*. 7 (2006) E4. doi:10.1208/pt070104.
- 411 [16] S.J. Macnaughton, I. Kikic, N.R. Foster, P. Alessi, A. Cortesi, I. Colombo, Solubility of Anti-  
412 Inflammatory Drugs in Supercritical Carbon Dioxide, *J. Chem. Eng. Data*. 41 (1996) 1083–  
413 1086. doi:10.1021/je960103q.
- 414 [17] L.A. Feldkamp, L.C. Davis, J.W. Kress, Practical cone-beam algorithm, *J. Opt. Soc. Am. A*. 1  
415 (1984) 612. doi:10.1364/JOSAA.1.000612.
- 416 [18] I. Kikic, M. Lora, A. Cortesi, P. Sist, Sorption of CO<sub>2</sub> in biocompatible polymers: experimental  
417 data and qualitative interpretation, *Fluid Phase Equilib.* 158-160 (1999) 913–921.  
418 doi:10.1016/S0378-3812(99)00063-1.
- 419 [19] P. Alessi, A. Cortesi, I. Kikic, F. Vecchione, Plasticization of polymers with supercritical  
420 carbon dioxide: Experimental determination of glass-transition temperatures, *J. Appl.*  
421 *Polym. Sci.* 88 (2003) 2189–2193. doi:10.1002/app.11881.
- 422 [20] I. Kikic, F. Vecchione, P. Alessi, A. Cortesi, F. Eva, N. Elvassore, Polymer Plasticization Using  
423 Supercritical Carbon Dioxide: Experiment and Modeling, *Ind. Eng. Chem. Res.* 42 (2003)  
424 3022–3029. doi:10.1021/ie020961h.
- 425 [21] A. Stassi, R. Bettini, A. Gazzaniga, F. Giordano, A. Schiraldi, Assessment of Solubility of  
426 Ketoprofen and Vanillic Acid in Supercritical CO<sub>2</sub> under Dynamic Conditions, *J. Chem. Eng.*  
427 *Data*. 45 (2000) 161–165. doi:10.1021/je990114u.
- 428 [22] M.L. Vueba, M.E. Pina, F. Veiga, J.J. Sousa, L.A.E.B. de Carvalho, Conformational study of  
429 ketoprofen by combined DFT calculations and Raman spectroscopy., *Int. J. Pharm.* 307  
430 (2006) 56–65. doi:10.1016/j.ijpharm.2005.09.019.
- 431 [23] L. Manna, M. Banchemo, D. Sola, A. Ferri, S. Ronchetti, S. Sicardi, Impregnation of PVP  
432 microparticles with ketoprofen in the presence of supercritical CO<sub>2</sub>, *J. Supercrit. Fluids*. 42  
433 (2007) 378–384. doi:10.1016/j.supflu.2006.12.002.

434